

Label-free Detection of Prostate Specific Antigen Using a Silicon Nanobelt Field-effect Transistor

Chi-Chang Wu¹, Tung-Ming Pan², Chung-Shu Wu¹, Li-Chen Yen³, Cheng-Keng Chuang⁴,
See-Tong Pang⁴, Yuh-Shyong Yang¹, Fu-Hsiang Ko^{1,*}

¹ Department of Materials Science and Engineering, Institute of Biological Science and Technology, National Chiao-Tung University, Hsinchu 300, Taiwan

² Department of Electronics Engineering, Chang Gung University, Taoyuan 333, Taiwan

³ Department of Electrophysics, National Chiao Tung University, Hsinchu 300, Taiwan

⁴ Division of Urology, Chang Gung Memorial Hospital, Taiyuan 333, Taiwan

*E-mail: fuhsiangko@yahoo.com.tw

Received: 16 February 2012 / Accepted: 3 April 2012 / Published: 1 May 2012

In this study, we proposed a silicon nanobelt field-effect transistor (FET) to detect prostate specific antigen (PSA). The nanobelt FET device displayed n-channel depletion characteristics. The immobilization of prostate specific antibody (anti-PSA) molecules was attached onto the nanobelt FET surface by using the aldehyde groups of glutaraldehyde linked to the amino groups of 3-aminopropyltriethoxysilane (APTES). The shift in the drain current vs time curves of a nanobelt FET biosensor revealed that the electrical signal had a logarithmic relationship with respect to the concentration of the PSA, and detection capability was estimated in the 5 pg/mL level. To enhance the sensitivity of a nanobelt FET biosensor, this biosensor was designed by inserting arginine molecules between glutaraldehyde and APTES. Therefore, the detection capability of the developed sensor was extended to 50 fg/mL. Also, the relationship between the current shift and the logarithm of PSA concentration was exhibited linearity in the range 50 fg/mL - 500 pg/mL. The excellent electrical results of this label-free PSA nanobelt FET biosensor suggested that such biosensor might be potentially useful tools for biological research and future prostate cancer screening.

Keywords: Nanobelt, Field-effect Transistor, Biosensor, Prostate Specific Antigen, Label-free Detection.

1. INTRODUCTION

Prostate specific antigen (PSA) is an enzyme produced in the ducts of the prostate and absorbed into the bloodstream. Such enzyme may become bound to two α 1-antichymotrypsin (ACT) and α 2-

macroglobulin proteins [1]. The "PSA test" measures the level of free and bound PSA in the blood. With benign prostate condition for patient, more portion of free PSA is observed, while cancer patient exhibits more portion of the bound form. The PSA concentration level in the serum is considered normal for an average man ranges from 0 to 4 ng/ml. PSA is usually a biological marker or a cancer marker and can be used to detect prostate disease. Currently, PSA level is a simple test to help the diagnosis of prostate cancer. PSA testing is also used to monitor the response of prostate cancer patients to ablative therapy such as radical prostatectomy. In this situation PSA should be undetectable, and a subsequent detectable level of PSA is a sign of disease recurrence. However, ultrasensitive assays that are capable of detecting concentrations of serum PSA in the low pg/ml range have been sought to facilitate earlier detection of recurrence [2]. Despite its wide use, PSA is not a cancer-specific marker, and other non-cancerous diseases of the prostate, such as benign prostatic hyperplasia (BPH), can also result in increased release of PSA into the circulation [3]. The development of ultrasensitive FET (field-effect transistor) biosensor that is affordable to distinguish between different isoforms of PSA, such as the ratio of free PSA to bound PSA, is inevitable for future disease diagnosis.

Trace levels of PSA are naturally found in the serum because prostate tumor growth usually causes the release of high concentrations of PSA into the circulatory system [3]. The use of PSA testing has aided the prediction of prostate cancer risk and treatment outcome. It is important to develop an ultrasensitive and selective biological sensor for PSA detection. An ultrasensitive biological detection system that allows the early detection of prostate cancer is expected to improve preventative healthcare. At present, the most widespread techniques for detecting prostate cancer are based on the enzyme-linked immunosorbent assay (ELISA). The ELISA method determines the PSA level in a sample through the magnitude of a fluorescence signal; its limitations include the need for a fluorescent label and relatively insensitive detection. As to the PSA detection, the development of real-time, high-sensitive, and label-free sensing devices that overcome the drawbacks of ELISA-based method remains a considerable challenge [4-5]. Recently, biomolecule sensors based on quasi one-dimensional semiconductor nanostructures, such as nanotubes, nanowires, and nanobelts, have attracted considerable attention because of their distinct electrical, optical, and magnetic properties [5-8]. Nanostructural materials have attracted much more attentions due to its unique character on various fields of application [9-12]. The large surface-to-volume ratios and high selective binding of charged biomolecules onto these nanostructure surfaces can result in significant changes of electronic conductance in the channel of the nanostructure [13-14]. In this paper, we develop a silicon nanobelt FET biosensor to detect the level of PSA. In order to enhance the method sensitivity, the molecular assembly technique is developed to immobilize more antibody and antigen. By using this novel technique, an ultrahigh-sensitive, label-free and real-time detection of prostate-specific molecule can be achieved.

2. EXPERIMENTAL

2.1 Fabrication of Si nanobelt FET devices

The silicon nanobelt FET devices were fabricated by using a n-doped silicon-on-insulator (SOI) substrate as shown in Fig. 1a. A commercially available 6-in. (100) SOI wafers with 500Å

silicon and 1500Å buried oxide layers were used for a silicon nanobelt FET fabrication. After a standard cleaning process, the stacked films of tetraethylorthosilicate (TEOS)-oxide and silicon nitride were deposited sequentially as the masking layer for LOCOS process.

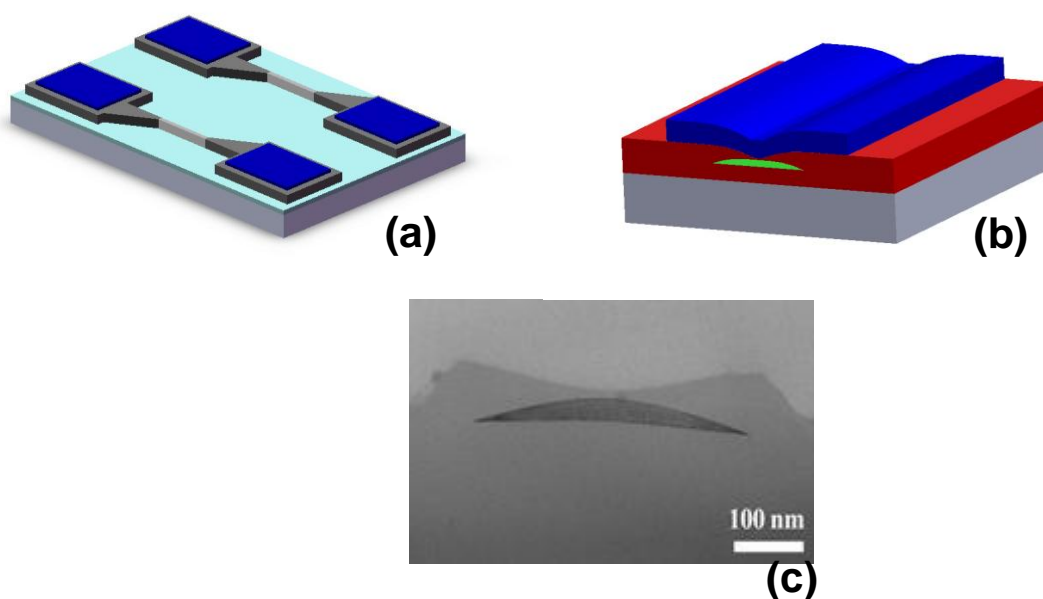


Figure 1. Schematic representation of (a) the Si nanobelt FET and (b) the shrunk nanobelt after LOCOS. (c) Cross-sectional TEM images of the nanobelt after performing 150 nm-thick oxidation steps.

The underlying layer of TEOS-oxide was used to release the transition of stresses between the silicon substrate and nitride film. Then, the active region (nanobelt), source, and drain electrodes were formed on the silicon nitride/pad Si dioxide by using optical lithography and plasma etching system. The silicon dioxide was thermally grown to oxidize the exposed silicon. Subsequently, the residue silicon nitride film was removed by phosphoric acid solution.

The source and drain regions were defined by using an optical lithography and ion implantation with a dosage energy of $5 \times 10^{15} \text{ cm}^{-2}$ and 20 keV from an arsenic ion beam, respectively, followed by rapid thermal annealing at 1050°C for 30 s in a nitrogen ambient.

After implantation process, the Al-Si-Cu alloy metallization was performed to define the contact pad. Finally, the silicon dioxide and nitride layers were then deposited to passivate the surface, and the detection region of the FET was etched back for the purpose of biomolecule detection. Fig. 1b and c shows the schematic representation of the Si nanobelt FET structure and the cross-sectional TEM image of the nanobelt, respectively.

2.2 Surface immobilization of silicon nanobelt FET biosensors

Before the device surface modification and electrical measurement, each of these samples was cleaned in acetone and ethanol mixing solution. Then, self-assembled monolayers were formed on the

surface of chip by immersing sample into a solution of 10 % APTES aqueous for 30 min, washed with DI water, and heated at 120°C for 30 min.

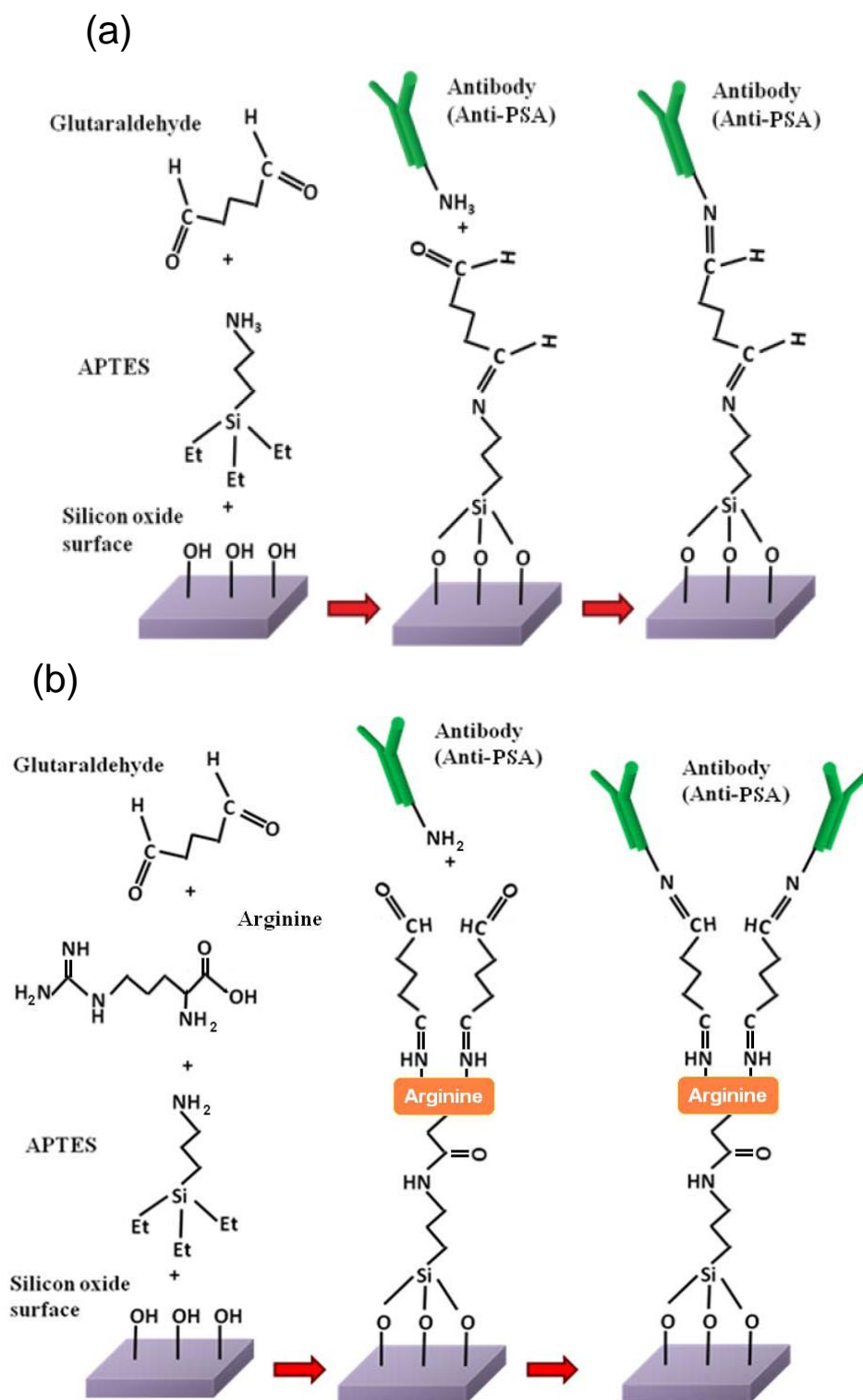


Figure 2. (a) The Si nanobelt presenting a native oxide on the surface was reacted with APTES, glutaraldehyde, and anti-PSA. (b) The Si nanobelt presenting a native oxide on the surface was reacted with APTES, arginine, glutaraldehyde, and anti-PSA.

The sample was subsequently rinsed with glutaraldehyde in phosphate buffered saline. Next, glutaraldehyde was linked to the amino groups to present aldehyde groups from the surface, as shown in Fig. 2a. Hereafter, the chips were immersed in prostate specific antibody (anti-PSA) solution overnight at 4°C and blocking the non-specific reactive sites by using 1% bovine serum albumin (BSA) solution. Each step was washed with DI water and dried with ambient nitrogen. Then, anti-PSA was linked to the aldehyde groups to form a FET biosensor.

To improve the sensitivity of a nanobelt FET biosensor, we employed the arginine molecules linking between APTES and glutaraldehyde in Fig. 2b. After APTES formed on the surface of this biosensor device, the sample was then soaked in 25 mg/ml arginine solution for 30 min. In this case, amides from carboxylic acids of arginine reacted with the amines group of APTES. Sample was heated at 120°C and immersed into arginine solution quickly. Next, sample was subsequently rinsed with 2.5% glutaraldehyde in phosphate buffered saline. At this stage, amino groups were presented as terminal units from the surface. Next, glutaraldehyde was linked to more amino groups to demonstrate aldehyde groups from the surface. Thereafter, the chips were immersed in each anti-PSA solution overnight and blocking the non-specific reactive sites by using 1 % BSA solution. Each step was washed by DI water and dried in ambient nitrogen. Figure 2b illustrates the preparation of the novel immobilization method.

After the attachment of anti-PSA molecule, the cancer marker PSA was reacted to bind with the anti-PSA molecule from the nanobelt FET surface. PSA solutions with various concentrations (50 fg/mL ~ 5 ng/mL) were prepared in the PBS solution and the pH level of each analyte was checked to be in the same by a pH meter tool. The PBS solution was injected into the microfluidic channel run through the nanobelt FET detection region to reduce the influence of buffer solution to the sensor. The real-time electrical response of the nanobelt FET sensor was obtained by the microfluidic system and Agilent 4156C.

3. RESULTS AND DISCUSSION

3.1 Electrical characteristics of Si nanobelt FET devices

Figure 3 presents the electrical characteristic of the fabricated nanobelt FET device. The drain current (I_D) versus gate voltage (V_G) dependence for drain voltage (V_D) at 0.5 and 1V is shown in Fig. 3a, and the I_D - V_D for varying V_G in Fig. 3b. The current flowing through the nanobelt channel between the source and drain electrodes could be switched “on” and “off” at various backside gate potentials. At a negative gate bias, the channel conduction (I_D) is very low. If a positive voltage is applied to the gate, many electron carriers are induced in the n-channel site for this device. In general, a backside gate applied a bias voltage to the nanobelt affects the energy barrier of channel for the charge carriers. This applied voltage ensures the device operation under the optimal condition to produce a larger current shift. The sub-threshold swing (SS) of a nanobelt FET device is about 268 mV/decade, which is much better than previous device [15]. The I_{on}/I_{off} current ratio of this device is approximately six orders of magnitude, suggesting improved practicality of the fabricated biosensors. The threshold

voltage (V_t) is about -1 V. The dependence of the I_D value on the applied gate voltage implies that the nanobelt FET sensors could be fine-tuned to optimal conditions to sense biomolecules due to the change in the surface charge.

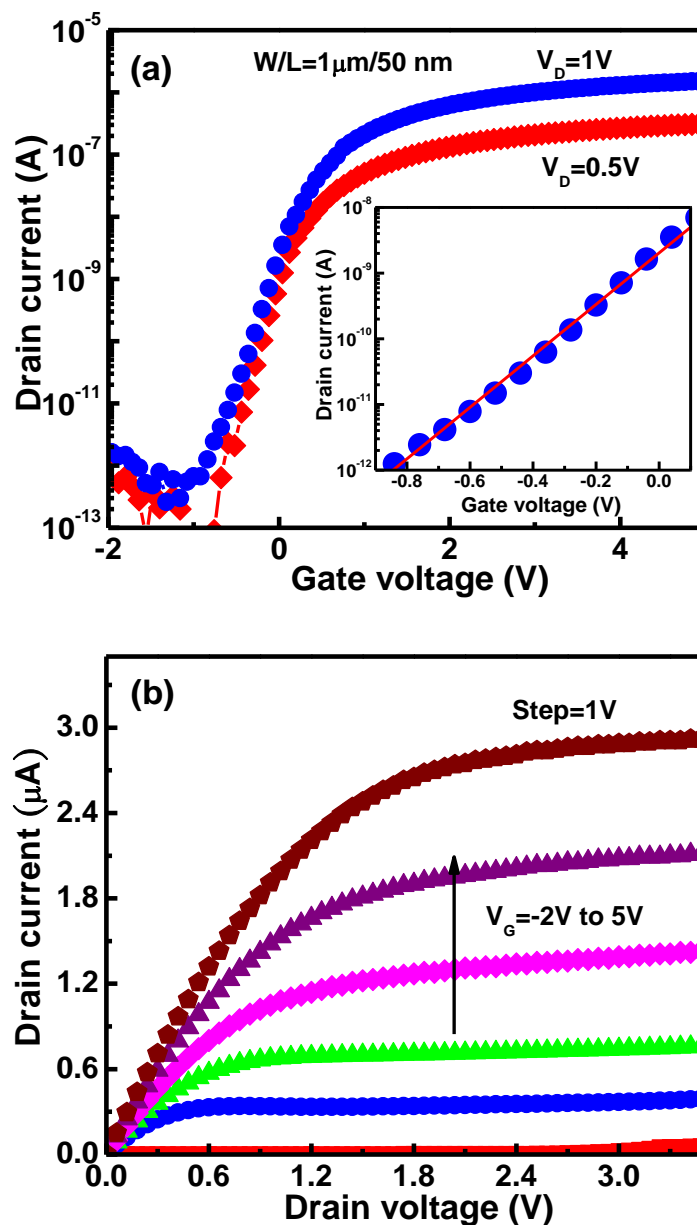


Figure 3. Electrical performance of the Si nanobelt FET device. (a) I_D - V_G dependence for $V_D = 0.5$ (red) and 1 V (blue). Inset: The subthreshold swing in subthreshold regime. (b) I_D - V_D curves of the nanobelt FET device at an applied gate voltage from -2 to 5 V with 1 V step.

3.2 Application of Si nanobelt FET devices

The nanobelt FET device is used as a biomolecule sensor for prostate cancer screening. The PSA is currently the best single test for prostate cancer screening. It has been reported that the amount

of serum PSA is directly correlated to the prostate cancer [2]. PSA antigen with various concentrations, including 5 pg/mL, 50 pg/mL, 500 pg/mL, and 5 ng/mL, respectively, is injected into the developed biosensor (without arginine bound) and continuously monitored its response. The relationship between PSA concentration and drain current is shown in Fig. 4a.

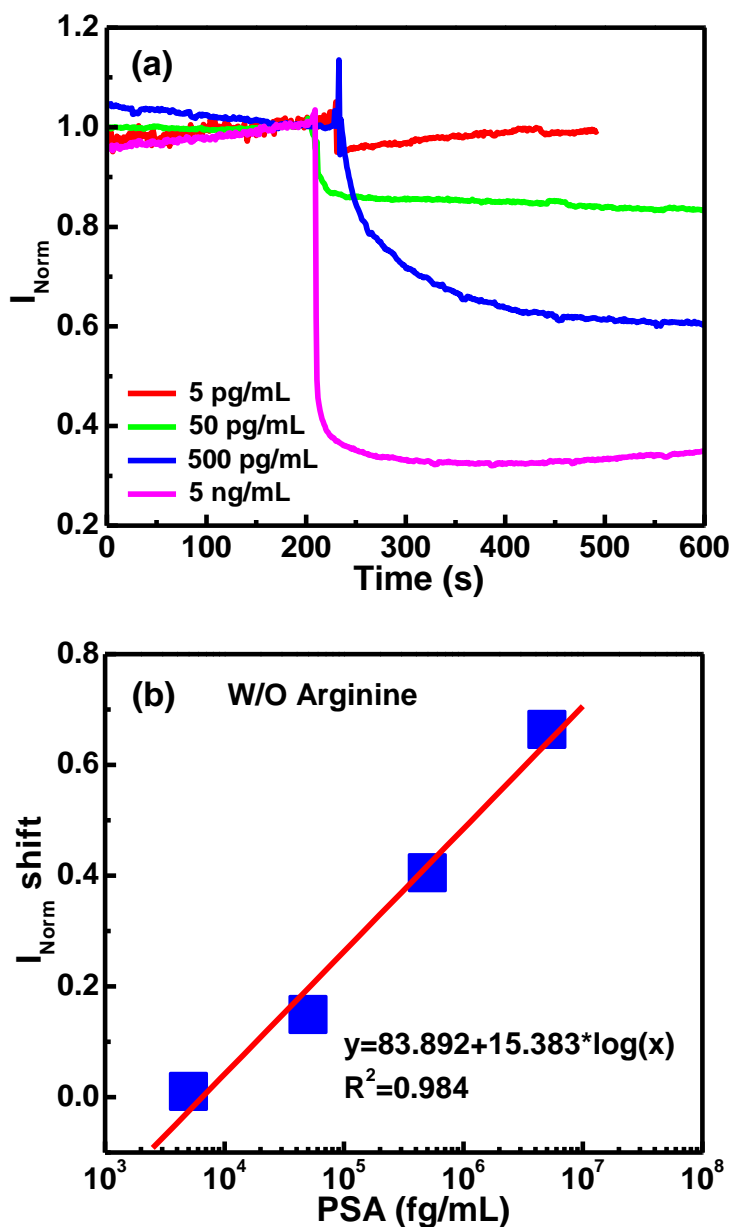


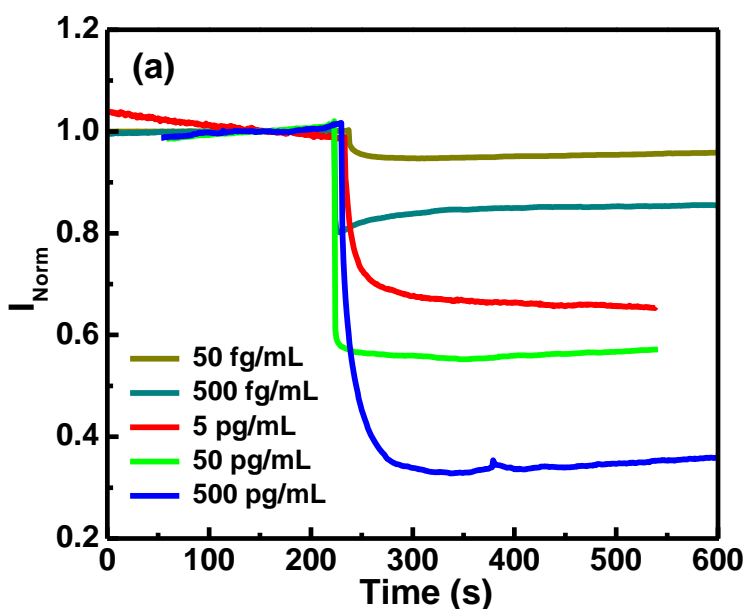
Figure 4. (a) Current response of the nanobelt FET biosensor (without arginine immobilization) for various PSA concentrations from 5 pg/mL to 5 ng/mL. (b) Normalized current shift as a function of PSA concentration for a nanobelt FET biosensor.

In Fig. 4b, the linear fitting for the calibration curve is $y = 15.383 \cdot \log(x) + 83.892$, with a correlation coefficient of 0.984. The higher concentration of PSA antigen is injected into the sensor, and the more decrease in drain current is monitored. This observation is attributed to the cause from

the negative charge character of the PSA antigen. The increase in negative charge hinders the conducting channel of such a nanobelt FET biosensor, and hence decreases the drain current. Although the sensitivity of PSA detection for this biosensor can attain a level of pg/mL for clinical applications, concentrations of serum PSA in the low fg/ml region should be also detected to facilitate earlier detection of prostate cancer patients' recurrence after radical prostatectomy.

3.3 Amplification of Si nanobelt FET sensor from arginine immobilization

We have enhanced this biosensor sensitivity by using arginine as an effective linker between the APTES and glutaraldehyde. The silica surface modification with APTES followed by glutaraldehyde activation and antibody attachment is a well-known procedure [16]. However, to the best of our knowledge, this method has not been applied for FET-based biosensor. When antibody molecules are covalently attached to silica through APTES, a large portion of its binding sites seems very close to the silica surface. The vicinity of a solid surface to the antigen binding sites may hinder the correct binding, leading to the decrease in the antibody activity. In order to provide the effective space region for the biosensor, we propose a novel surface immobilization strategy by inserting arginine molecules between the APTES and glutaraldehyde. Since arginine molecule carries abundant amino terminals and can easily react with glutaraldehyde via Schiff base reaction. Hence, the surface effect of recognition site for antibody is avoided, and more accessible site to the antigen from the bound antibody can be predicted. Insertion of the arginine molecule between the APTES and glutaraldehyde also can provide more positive charge surrounding to preserve the biosensor at pH 7.4. Because the interaction between the ligand and receptor is the dominant electrostatic effect by Coulomb's effect, the tight-binding ligands would be constructed very large charges to compensate charges at the active site [17]. In addition, the antigen, which carries native negative charges in solution, is attracted by positive charge of arginine.



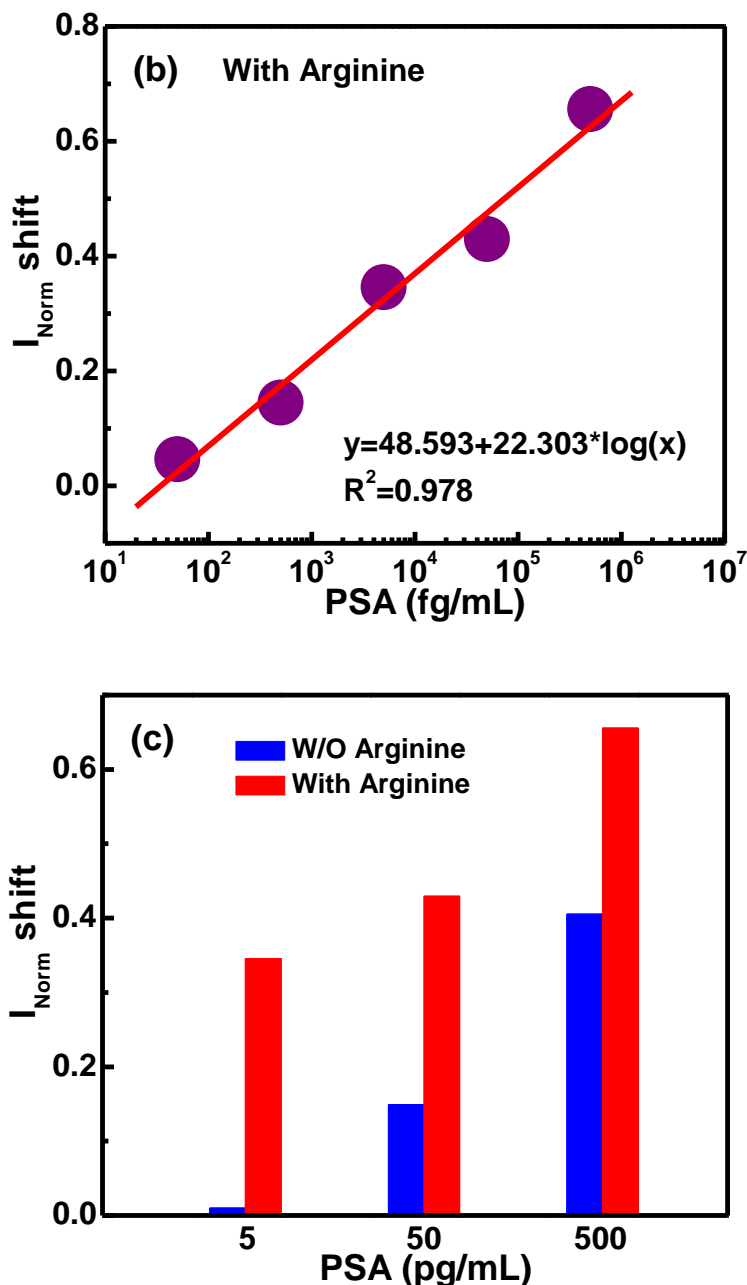


Figure 5. (a) Current response of the nanobelt FET biosensor using arginine immobilization for various PSA concentrations from 50 fg/mL to 500 pg/mL. (b) Normalized current shift as a function of PSA concentration for a nanobelt FET biosensor using arginine. (c) The effect of arginine molecule on the current shift for three PSA concentration levels.

Moreover, the short length of arginine is placed inside a Debye length, its effect on the mobile charges of the material is not significant. An attracting force occurs between two charged antigen and arginine to compress the gap of nanobelt channel and antigen. Consequently, more biomolecules can be trapped by inserting an arginine modification to amplify the detection signal.

Figure 5a shows the relationship between PSA (antigen) concentration (from 50 fg/mL to 500 pg/mL) and drain current for a nanobelt FET biosensor from an arginine immobilization. The observed concentration-dependent decrease in I_D is consistent with the total binding of a negatively charged PSA

antigen to antibody receptor for the n-channel FET devices. The normalized current shift exhibits a linear trend with logarithmic PSA concentration, as indicated in Fig. 5b. The linear fitting for the calibration curve is $y = 22.303 \cdot \log(x) + 48.593$, with a correlation coefficient of 0.978. Significantly, this slope (response or sensitivity) is higher than the slope from Fig. 4b. As the signal response from the assistance of arginine molecule, Figure 5c compares the signal response from three different concentration levels. Obviously, the initial current is very small for 5 pg/mL PSA from the sensor without arginine immobilization. This observation verifies the improvement of surface immobilization with the arginine molecule. Moreover, the biosensor with arginine immobilization can reach the lower PSA concentration region detection. This finding provides an effective means for future FET biosensor application. The excellent electrical performance of this label-free PSA nanobelt FET biosensor demonstrates the potential feasibility for future prostate cancer detection.

4. CONCLUSIONS

We have successfully developed a label-free nanobelt FET biosensor that allows efficient PSA biosensing. The nanobelt FET device is fabricated and operated under n-channel depletion characteristics. The aldehyde groups from glutaraldehyde linked to the amino groups of APTES is attached on the biosensor surface to immobilize anti-PSA molecules. The output signal of the developed FET biosensor without arginine amplification is linearly increase with the logarithm of PSA concentration in the range from 5 to 5000 pg/mL. To improve the sensing sensitivity of PSA molecule, this biosensor is improved by inserting arginine molecule between glutaraldehyde and APTES. The lowest readable signal from this sensor is 50 fg/mL for PSA. Because this label-free FET biosensor demonstrates the ability to detect the lower concentration of PSA molecule, such biosensor is demonstrated the potentially useful platform for biological research, prostate cancer screening and palliative care for prostate cancer patients in the future.

ACKNOWLEDGMENTS

The authors would like to thank the Chang Gung Memorial Hospital and the National Science Council of the Republic of China, Taiwan, for financially supporting this research under contract of CMRPD290031, CMRPD290032 and NSC 98-2113-M-009-017, respectively.

References

1. H. Lilja, D. Ulmert, A. J. Vickers, *Nat. Rev. Cancer*, 8 (2008) 268.
2. D. A. Healy, C. J. Hayes, P. Leonard, L. McKenna, R. O'Kennedy, *Trends Biotechnol.*, 25 (2007) 125.
3. U. H. Stenman, J. Leinonen, W.-M. Zhang, P. Finne, *Semin. Cancer Biol.*, 9 (1999) 83.
4. K. L. Moore, A. F. Dalley, A. M. R. Agur, P. W. Tank, T. R. Gest, *Clinically Oriented Anatomy*, Lippincott Williams & Wilkins, Baltimore (1999).
5. X. Tang, S. Bansaruntip, N. Nakayama, E. Yenilmez, Y.-L. Chang, Q. Wang, *Nano Lett.*, 6 (2006) 1632.

6. F. Patolsky, G. Zheng, C. M. Lieber, *Nature Protocols*, 1 (2006) 1711.
7. Y. Cheng, P. Xiong, C. S. Yun, G. F. Strouse, J. P. Zheng, R. S. Yang, Z. L. Wang, *Nano Lett.*, 8 (2008) 4179.
8. M. Zhang, F. Cheng, z. Cai, H. Yao, *Int. J. Electrochem. Sci.*, 5 (2010) 1026.
9. D. Wei, G. Amaratunga, *Int. J. Electrochem. Sci.*, 2 (2007) 897.
10. C.-C. Wu, Y.-J. Tsai, M.-C., Chu, S.-M. Yang, F.-H. Ko, P.-L. Liu, W.-L. Yang, H.-C. You, *Appl. Phys. Lett.*, 92 (2008) 123111.
11. C.-C. Lin, F.-H. Ko, C.-C. Chen, Y.-S. Yang, F.-C. Chang, C.-S. Wu, *Electrophoresis*, 30 (2009) 3189.
12. H. Karami, A. Kaboli, *Int. J. Electrochem. Sci.*, 5 (2010) 706.
13. C.-H. Lin, C.-Y. Hsiao, C.-H. Hung, Y.-R. Lo, C.-C. Lee, C.-J. Su, H.-C. Lin, F.-H. Ko, T.-Y. Huang, Y.-S. Yang, *Chem. Commun.*, (2008) 5749.
14. C.-Y. Hsiao, C.-H. Lin, C.-H. Hung, C.-J. Su, Y.-R. Lo, C.-C. Lee, H.-C. Lin, F.-H. Ko, T.-Y. Huang, Y.-S. Yang, *Biosens. Bioelectron.*, 24 (2009) 1223.
15. C.-C. Wu, F.-H. Ko, Y.-S. Yang, D.-L. Hsia, B.-S. Lee, T.-S. Su, *Biosens. Bioelectron.*, 25 (2009) 820.
16. H. H. Weetall, *Methods Enzymol.*, 44 (1976) 134.
17. L.Y. Zhang, E. Gallicchio, R. A. Friesner, R. M. Levy, *J. Comput. Chem.*, 22 (2001) 591.